JOC Article

Conformational Landscape of *meso*-(1,3-Dithian-2-yl)porphyrins

Philipp Wacker,[†] Katja Dahms,[‡] Mathias O. Senge,[‡] and Erich Kleinpeter*,[†]

Institut für Chemie, Universität Potsdam, Karl-Liebknecht-Strasse 24-25, D-14476 Golm, Germany, and School of Chemistry, SFI Tetrapyrrole Laboratory, University College Dublin, Trinity College, Dublin 2, Ireland

kp@chem.uni-potsdam.de

Received April 25, 2007

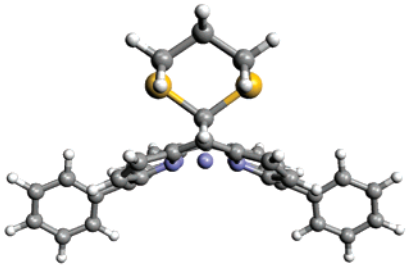

Rotational transition state of 4

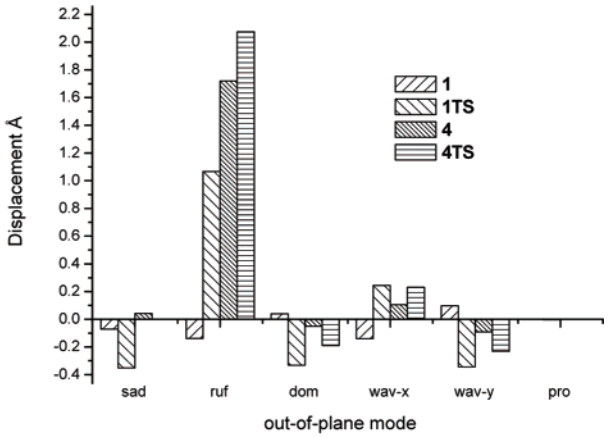

NSD-analysis

An investigation of the conformational landscape of 1,3-dithian-2-yl bearing porphyrins and the rotational behavior of the dithianyl substituents in *meso* position was carried out by variable-temperature (VT) NMR spectroscopy. Additionally, theoretical results for alternative conformations and energy barriers were obtained by molecular modeling. The study revealed different NH trans tautomers with regard to the orientation of the dithianyl ligands for the free base porphyrins **1**−**3**. Relatively ruffled porphyrin core conformations were established for the transition states of the dithianyl rotation, resulting in a lower rotational energy barrier for the nickel(II) complex **4** compared to that of the free base systems. The data obtained and the first depiction of a rotational transition state for the rotation of bulky *meso*-alkyl substituents illustrate the close structural interplay between *meso*-alkyl substituents and the macrocycle conformation in porphyrins.

Introduction

Porphyrins are among the most widely investigated natural and synthetic ligand systems and have served to establish many fundamental aspects of macrocycle and aromatic chemistry.[1] In the past, many studies have addressed the influence of the core conformation (e.g., the central metal and axial ligands on the ligand properties).[2] Likewise, the peripheral substituents at the meso and β-positions have a considerable impact on the physical and chemical properties of a porphyrin, and conformational aspects are important for the in vivo regulation of tetrapyrrole cofactors.[3,4] This is not only a result of the electronic and steric effects of the substituents, but also the orientation and conformation of the substituent can affect the porphyrin core. Porphyrin systems with *meso*-aryl substituents have been investigated in detail. Especially for porphyrins with four identical *meso*-aryl substituents a significant body of information

[†] Universität Potsdam.

[‡] Trinity College Dublin.

(1) *The Porphyrin Handbook;* Kadish, K. M., Guilard, R., Smith, K. M., Eds.; Academic Press: San Diego, CA, 2000.

(2) (a) Scheidt, W. R.; Lee, Y. J. *Struct. Bonding (Berlin)* **1987**, *64*, 1−70. (b) Scheidt, W. R. In *The Porphyrin Handbook;* Kadish, K. M., Guilard, R., Smith, K. M., Eds.; Academic Press: San Diego, CA, 2000; Vol. 3, pp 49−112.

(3) (a) Senge, M. O. *J. Photochem. Photobiol., B* **1992**, *16*, 3−36. (b) Ravikanth, M.; Chandrashekar, T. K. *Struct. Bonding (Berlin)* **1995**, *82*, 105−188. (c) Senge, M. O. In *The Porphyrin Handbook;* Kadish, K. M., Guilard, R., Smith, K. M., Eds.; Academic Press: San Diego, CA, 2000; Vol. 1, pp 239−347. (d) Senge, M. O. *Chem. Commun.* **2006**, *3*, 243−256. (e) Senge, M. O. *Acc. Chem. Res.* **2005**, *38*, 733−743.

(4) Shelnutt, J. A.; Song, X.-Z.; Ma, J.-G.; Jia, S.-L.; Jentzen, W.; Medforth, C. J. *Chem. Soc. Rev.* **1998**, *27*, 31−42.

10.1021/jo0708700 CCC: $37.00
Published on Web 07/12/2007

is available.[5,6] In contrast, much less is known about the rotational behavior of *meso*-alkyl substituents.

For example, Veyrat et al. compared zinc(II) and nickel(II) complexes of 5,10,15,20-tetracyclohexylporphyrin with variable-temperature (VT) NMR spectroscopy and observed a different signal pattern in the proton spectra at low temperature and different energy barriers for the cyclohexyl rotation.[7] The nickel-(II) complex exhibited a splitting of the ^{1}H NMR resonances for the *meso*-cyclohexyl group, whereas this pattern was absent in the spectra of the less distorted zinc analogue. It was concluded that different core conformations are responsible for this behavior. In ^{1}H NMR studies of a series of high-spin chloro-(*meso*-tetraalkylporphyrinato)iron(III), Ikeue et al. investigated the 180° rotation of the alkyl groups.[8] For the isopropyl groups, a $\Delta G^{\ddagger}$ value of 8.9 kcal mol^{-1} was determined. This represents a decrease in $\Delta G^{\ddagger}$ by 2.5 kcal mol^{-1} for the change from cyclohexyl to isopropyl. The smaller rotation barrier was correlated to the deformation of the porphyrin ring. Wołowiec et al. used NMR spectroscopy and molecular mechanics calculations to study the electronic properties, structures, and symmetry of iron(III) complexes of 5,10,15,20-tetracyclohexylporphyrin.[9]

Tetrapyrroles are vitally important natural products, and many conformational investigations have been performed. These include the studies on nonplanar porphyrins and the in vivo physicochemical consequences of macrocycle distortion as well as examinations of the conformation of heme and hemelike molecules.[10] Thus far, only *meso*-aryl-substituted porphyrins have been explored in detail in both the solid and solution states. For the *meso*-alkyl-substituted porphyrins, primarily solid-state data are available, and the data's relevance for the situation in vivo or in pigment−protein complexes is limited.[11]

To elucidate the influence of alkyl substituent orientation and conformation on the macrocycle, we have chosen the *meso*-dithianylporphyrins **1**−**4** for a comparative NMR and computational study (Figure 1). The dithianyl group is an important synthon in organic chemistry, notably for Umpolung reactions.[12] In porphyrin chemistry, it offers the possibility to circumvent some of the limitations of classic Vilsmeier reactions for the preparation of formylporphyrins.[13,14] Additionally, the presence of the sulfur atom in close vicinity to the porphyrin macrocycle might serve as a model for the influence of thio residues in porphyrin−protein complexes either covalent and noncovalent interactions.[4,15]

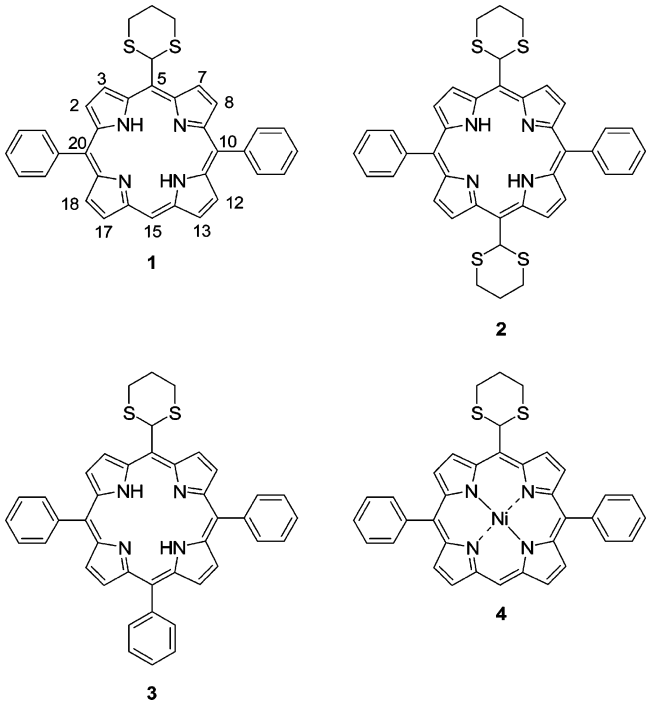

FIGURE 1. Porphyrins **1**−**4**.

Here, we report on the rotational behavior of the dithianyl moiety in differently substituted porphyrins and describe its influence on the NH tautomerism and the role of core deformation on the rotational barriers and vice versa.

Results and Discussion

Variable-Temperature ^{1}H NMR Spectra. To study the conformational behavior and to gain experimental results for

(5) (a) Eaton, S. S.; Eaton, G. R. *J. Am. Chem. Soc.* **1975**, *97*, 3660−3666. (b) Eaton, S. S.; Eaton, G. R. *J. Am. Chem. Soc.* **1977**, *99*, 6594−6599. (c) Crossley, M. J.; Field, L. D.; Forster, A. J.; Harding, M. M.; Sternhell, S. *J. Am. Chem. Soc.* **1987**, *109*, 341−348. (d) Noss, L.; Liddell, P. A.; Moore, A. L.; Moore, T. A.; Gust, D. *J. Phys. Chem. B* **1997**, *101*, 458−465. (e) Okuno, Y.; Kamikado, T.; Yokoyama, S.; Mashiko, S. *J. Mol. Struct.: THEOCHEM* **2002**, *594*, 55−60. (f) Medforth, C. J.; Haddad, R. E.; Muzzi, C. M.; Dooley, N. R.; Jaquinod, L.; Shyr, D. C.; Nurco, D. J.; Olmstead, M. M.; Smith, K. M.; Ma, J.-G.; Shelnutt, J. A. *Inorg. Chem.* **2003**, *42*, 2227−2241. (g) Rosa, A.; Ricciardi, G.; Baerends, E. J. *J. Phys. Chem. A* **2006**, *110*, 5180−5190.

(6) Medforth, C. J. In *The Porphyrin Handbook;* Kadish, K. M., Guilard, R., Smith, K. M., Eds.; Academic Press: San Diego, CA, 2000; Vol. 5, p 72 and references therein.

(7) (a) Veyrat, M.; Ramasseul, R.; Marchon, J.-C.; Turowska-Tyrk, I.; Scheidt, W. R. *New J. Chem.* **1995**, *19*, 1199−1202. (b) Veyrat, M.; Ramasseul, R.; Turowska-Tyrk, I.; Scheidt, W. R.; Autret, M.; Kadish, K. M.; Marchon, J.-C. *Inorg. Chem.* **1999**, *38*, 1772−1779.

(8) Ikeue, T.; Ohgo, Y.; Uchida, A.; Nakamura, M.; Fujii, H.; Yokoyama, M. *Inorg. Chem.* **1999**, *38*, 1276−1281.

(9) Wołowiec, S.; Latos-Grażyński, L.; Toronto, D.; Marchon, J.-C. *Inorg. Chem.* **1998**, *37*, 724−732.

(10) (a) Huber, R. *Eur. J. Biochem.* **1990**, *187*, 283−305. (b) Barkigia, K. M.; Nurco, D. J.; Renner, M. W.; Melamed, D.; Smith, K. M.; Fajer, J. *J. Phys. Chem. B* **1998**, *102*, 322−326. (c) Nurco, D. J.; Smith, K. M.; Fajer, J. *Chem. Commun.* **2002**, *24*, 2982−2983. (d) Barkigia, K. M.; Renner, M. W.; Senge, M. O.; Fajer, J. *J. Phys. Chem. B* **2004**, *108*, 2173−2180. (e) Martí, M. A.; Capece, L.; Crespo, A.; Doctorovich, F.; Estrin, D. A. *J. Am. Chem. Soc.* **2005**, *127*, 7721−7728. (f) Schneider, S.; Sharp, K. H.; Barker, P. D.; Paoli, M. *J Biol. Chem.* **2006**, *281*, 32606−32610. (g) Rutkowska-Zbik, D.; Witko, M.; Stochel, G. *J Comput. Chem.* **2007**, *28*, 825−831.

(11) (a) Ohgo, Y.; Ikeue, T.; Takahashi, M.; Takeda, M.; Nakamura, M. *Eur. J. Inorg. Chem.* **2004**, 798−809. (b) Pellerito, C.; Scopelliti, M.; Fiore, T.; Nagy, L.; Barone, G.; Abbate, M.; Stocco, G. C.; Pellerito, L. *J. Organomet. Chem.* **2006**, *691*, 1573−1583. (c) Sazanovich, I. V.; Galievsky, V. A.; van Hoek, A.; Schaafsma, T. J.; Malinovskii, V. L.; Holten, D.; Chirvony, V. S. *J. Phys. Chem. B* **2001**, *105*, 7818−7829. (d) Hayashi, S.; Kato, S. *J. Phys. Chem. A* **1998**, *102*, 3333−3342. (e) Evans, J. S.; Musselman, R. L. *Inorg. Chem.* **2004**, *43*, 5613−5629. (f) Senge, M. O.; Renner, M. W.; Kalisch, W. W.; Fajer, J. *J. Chem. Soc., Dalton Trans.* **2000**, *3*, 381−385.

(12) (a) Beer, R. J. S.; Harris, D.; Royall, D. J. *Tetrahedron Lett.* **1964**, *23*−*24*, 1531−1536. (b) Carlson, R. M.; Helquist, P. M. *Tetrahedron Lett.* **1969**, *3*, 173−176. (c) Seebach, D. *Synthesis* **1969**, *1*, 17−36. (d) Page, P. C. B.; Van Niel, M. B.; Prodger, J. C. *Tetrahedron* **1989**, *45*, 7643−7677. (e) Seebach, D.; Corey, E. J. *J. Org. Chem.* **1975**, *40*, 231−237.

(13) Saito, K.; Ohzone, Y.; Kondo, Y.; Ono, K.; Ohkita, M. *Heterocycles* **2004**, *62*, 773−778.

(14) Senge, M. O.; Hatscher, S. S.; Wiehe, A.; Dahms, K.; Kelling, A. *J. Am. Chem. Soc.* **2004**, *126*, 13634−13635.

(15) (a) Erman, J. E.; Vitello, L. B. *J. Biochem. Mol. Biol.* **1998**, *31*, 307−327. (b) Zederbauer, M.; Jantschko, W.; Neugschwandtner, K.; Jakopitsch, C.; Moguilevsky, N.; Obinger, C.; Furtmuller, P. G. *Biochemistry* **2005**, *44*, 6482−6491. (c) Latypov, R. F; Cheng, H.; Roder, N. A; Zhang, J.; Roder, H. *J. Mol. Biol.* **2006**, *357*, 1009−1025.

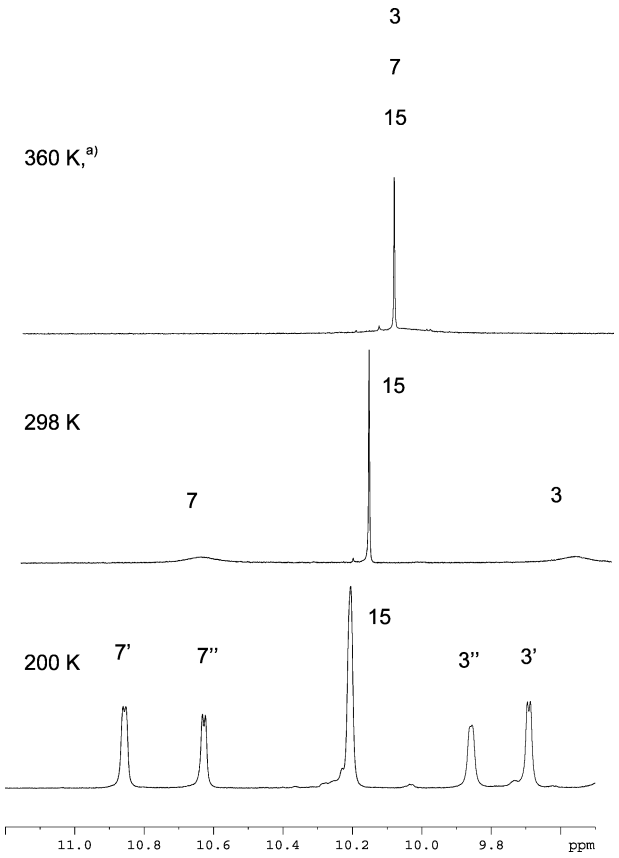

FIGURE 2. ^{1}H NMR spectra of protons H3/7/15 for porphyrin **1** at different temperatures in CD_2Cl_2. a) = $C_2D_2Cl_4$, δ TMS/500 MHz. Changes in the whole aromatic region are given in Figures S1−S4 in the Supporting Information.

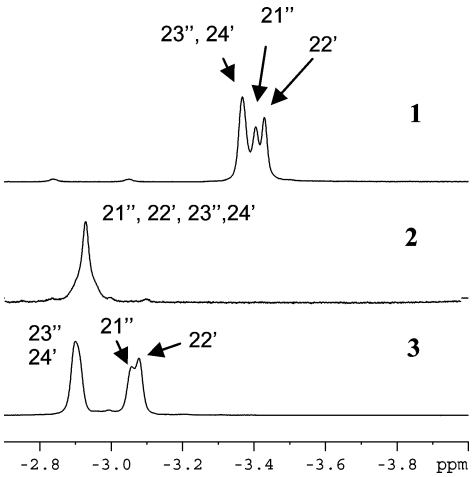

FIGURE 3. NH section of the ^{1}H NMR spectra of **1**−**3** at 200 K and 500 MHz.

energy barriers, we subjected compounds **1**−**4** to an ^{1}H NMR investigation at various temperatures. Changing the sample temperature had a considerable impact on the signal pattern for the β-proton resonances in the corresponding ^{1}H NMR spectra (Figures 2 and S1). Similarly, differences were observed for the NH proton resonances for the free base porphyrins **1**−**3** (Figure 3). To show the nature of these differences, the changes observed upon variation of the temperature are illustrated here exemplary for porphyrin **1**.

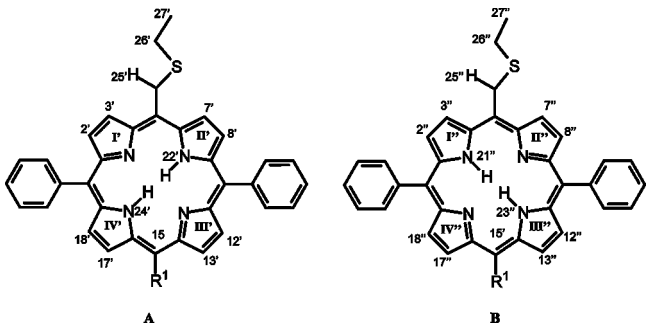

FIGURE 4. Two trans tautomers for **1**−**3**. The **B** tautomer is higher in energy. The schematic side view of the dithianyl moieties illustrates their orientations.

Parts of the ^{1}H NMR spectra containing the resonances of H3/7 in **1** for three characteristic temperatures are shown in Figure 2. Above the coalescence temperature of 334 K the ^{1}H NMR resonances of protons H3/7 are fused, and below it they split into two broad resonances. Further cooling of the sample causes decoalescence of each of these resonances into two sets, labeled as 3′/3″ and 7′/7″, respectively. At 200 K, four resonances with different intensities are observed for the β-protons adjacent to the dithianyl group. A similar splitting can be observed for the remaining β-protons of porphyrins **1**−**3** as well (Supporting Information Figure S1). In contrast, the signals for the β-protons of the nickel(II) complex **4** are split only once in the observed temperature range.

Figure 3 shows the observed NH signals of **1**−**3** at 200 K. By raising the temperature to room temperature (298 K), only a single resonance is observed for the NH protons at high field. Clearly these differences are a result of the NH tautomerism in the free base porphyrins **1**−**3** being fast on the NMR time scale. Lowering the temperature decelerates the inner proton hopping process, and the positions of the NH protons on the different pyrrole rings become distinguishable.[16] As shown in Figure 3, at 200 K three resonances are observed for porphyrins **1** and **3**. As a result of the symmetric substituent pattern, compound **2** exhibits a broadened single resonance for the inner protons.

Ground-State Conformations. To explain the results of the VT NMR data, two NH trans tautomers **A** and **B** (Figure 4) have to be assumed for the free base porphyrins **1**−**3**. This is a result of the restricted rotation of the dithianyl group. Further experimental proof for the existence of two different tautomers is obtained from the long-range COSY spectra of **1** at 200 K (Figure 5). The cross-peaks clearly enable the assignment of the NH resonances to the respective tautomeric forms.

An analysis of the accurate integration of the well-separated H3′/3″ and H7′/7″ resonances at 200 K indicates that the equilibrium between both tautomers is slightly shifted in favor of the **A** form. To establish a structural basis for the dominance of the **A** tautomers, the energy minima structures for porphyrins **1**−**3** were calculated. Thus, different orientations and conformation of the meso substituents and different trans tautomers (for **1**−**3**) were optimized, and the resulting global minima structures of the **A** tautomers are shown in Figure 6.

Noticeably, the porphyrin core in the free base compounds **1**−**3** adopts an almost planar conformation, whereas the

(16) (a) Storm, C. B.; Teklu, Y. *J. Am. Chem. Soc.* **1972**, *94*, 1745−1747. (b) Abraham, R. J.; Hawkes, G. E.; Smith, K. M. *Tetrahedron Lett.* **1974**, *16*, 1483−1486 (c) Eaton, S. S.; Eaton, G. R. *J. Am. Chem. Soc.* **1977**, *99*, 1601−1604.

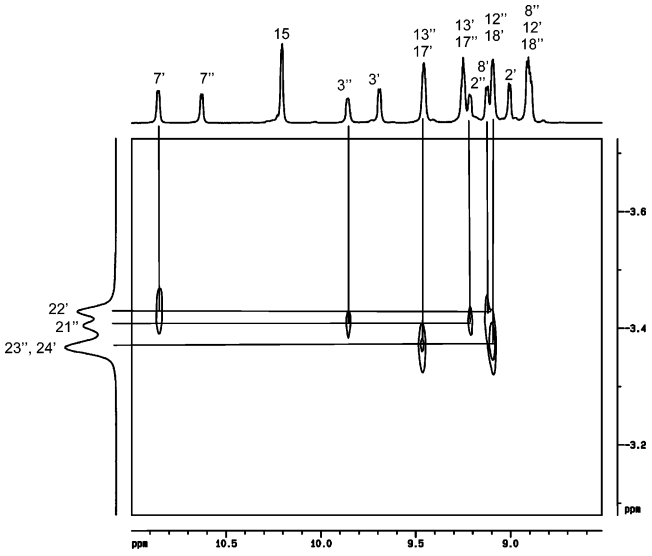

FIGURE 5. Long-range COSY of the ^{1}H NMR spectra of the β- and meso protons for porphyrin **1** at 200 K and 500 MHz.

TABLE 1. Experimental and Calculated Energy Differences between the Tautomeric Forms A and B (kJ/mol)

	exptl ΔG^0	calcd[a] ΔE
1	+0.27	+1.92
2	+0.3	+3.67
3	+0.4	+1.58

[a] B3LYP/6-31G**.

macrocycle core of the nickel(II) complex **4** reveals significant out-of-plane deformations. This is in agreement with a single-crystal X-ray structure of **2**, which exhibited a planar macrocycle for this compound in the solid state.[14] In the calculated structures, the dihedral angles between the porphyrin and phenyl least-squares planes fluctuate from 68 to 70°. As a result of conjugation effects, the 10- and 20-phenyl rings are parallel to each other to maximize conjugation. For porphyrin **3**, the angle between the plane of the 15-phenyl ring and the mean plane of the porphyrin macrocycle was calculated to be 62°. The tautomeric form **B**, characterized by H21 and H25 being localized in the same quadrant of the molecule, has a slightly higher energy than the **A** tautomers. The experimental and calculated energy differences are summarized in Table 1. This further supports the finding of a slight dominance for the **A** form in the spectra.

For free base **2**, three trans structures with similar energy could be calculated. The different forms are illustrated in Figure 7, and they are distinguished by the respective orientation of the additional dithianyl group in position 15. Thus, the presence of a second dithianyl residue imparts additional features on the spectra. As derived from ab initio calculations, structure **2A** is the lowest energy form. Tautomer **2B** is 3.6 kJ mol^{-1} higher in energy. In comparison, form **2C** was calculated to be 1.8 kJ mol^{-1} higher in energy. Thus, we conclude that only forms **2A** and **2C** contribute to the features observed in the NMR spectra giving rise to two signal sets. A structural basis for energy differences between the **A** and **B** tautomers can be found in the stretching of the porphyrin core along the N−H−H−N axis. The repulsion of the inner protons results in different spatial separations between proton 7′ and sulfur compared to that of H7″−S. For the **B** tautomers, the average H−S distance (2.7 Å) is shortened by approximately 0.1 Å compared to that of the **A** tautomers (2.8 Å).

TABLE 2. Experimental[a] and Calculated (in Italics)[b] ^{1}H Chemical Shifts (ppm) for the β-Protons H3′/3″ and H7′/7″

porphyrin	3′	3″	7′	7″
1	9.70	9.87	10.85	10.63
	9.59	*9.78*	*10.99*	*10.68*
2	9.63	9.79	10.72	10.49
	9.48	*9.66*	*10.81*	*10.50*
3	9.67	9.84	10.98	10.56
	9.50	*9.70*	*10.99*	*10.59*

[a] 200 K, CD_2Cl_2. [b] B3LYP//6-31G**.

However, the behavior of the proton resonances is based on not only the NH tautomerism but also two dynamic processes. The first dynamic process is indicated by the splitting of the initially single resonance for H3/7 and has its origin in the slowing of the rotation of the *meso*-dithianyl substituent. Lowering the temperature retards the rotation of the dithianyl group about the C5−C25 axes. The process becomes slow with respect to the NMR time scale, and the symmetry along the molecular axes 5/15 is lost. As a consequence, the respective β-protons become distinguishable. This effect is strongest for the adjacent protons H3/7 adjacent to the meso residue and is a result of intramolecular H_β−S bonding interactions. The signal for the H7 protons adjacent to the sulfur atoms is shifted to lower field in all four compounds (**1**−**4**). This result is confirmed by an NOE between proton H3 and H25. Furthermore, the agreement of calculated and experimentally obtained ^{1}H NMR chemical shifts for the β-protons H3 and H7 supports this finding (Table 2).

As described, the other dynamic process involves the inner proton hopping process and affects the second splitting of the β-proton resonances H3 and H7 of **1**−**3** into H3′/H3″ and H7′/H7″, respectively. As a result of the ring current, the β-proton signals on the pyrrole rings with NH units are shifted to lower field.[17] In addition, the β-proton resonances associated with the NH bearing rings are broadened as well. Additionally, this is a result of the ^{4}J coupling to the inner protons.[18] Compared to that of the pyrrolenine rings, the difference in the ^{1}H NMR chemical shift of the β-protons belonging to the inner proton bearing rings averages 0.2 ppm for compounds **1**−**3** (Table 2). Furthermore, the significant changes observed for the H3/H7 signals and the other β-proton resonances for H2/H8, H12/H18, and H13/H17 also become split as a consequence of the orientation of the dithianyl moiety. The splitting is less pronounced with increasing distance from the dithianyl moiety.

Macrocycle Inversion. As mentioned above, the signals originating from the dithianyl protons underwent no significant changes throughout the temperature range. This implies that macrocycle inversion of the nickel(II) complex **4** is either fast on the NMR time scale[19] and cannot be observed or does not take place. Typical activation energies for the inversion of highly substituted porphyrins reported in the literature (e.g., dodeca-

(17) Jusélius, J.; Sundholm, D. *Phys. Chem. Chem. Phys.* **2000**, *2*, 2145−2151.

(18) Storm, C. B.; Teklu, Y.; Sokoloski, E. A. *Ann. N.Y. Acad. Sci.* **1973**, *206*, 631−640.

(19) Medforth, C. J.; Senge, M. O.; Forsyth, T. P.; Hobbs, J. D.; Shelnutt, J. A.; Smith, K. M. *Inorg. Chem.* **1994**, *33*, 3865−3872.

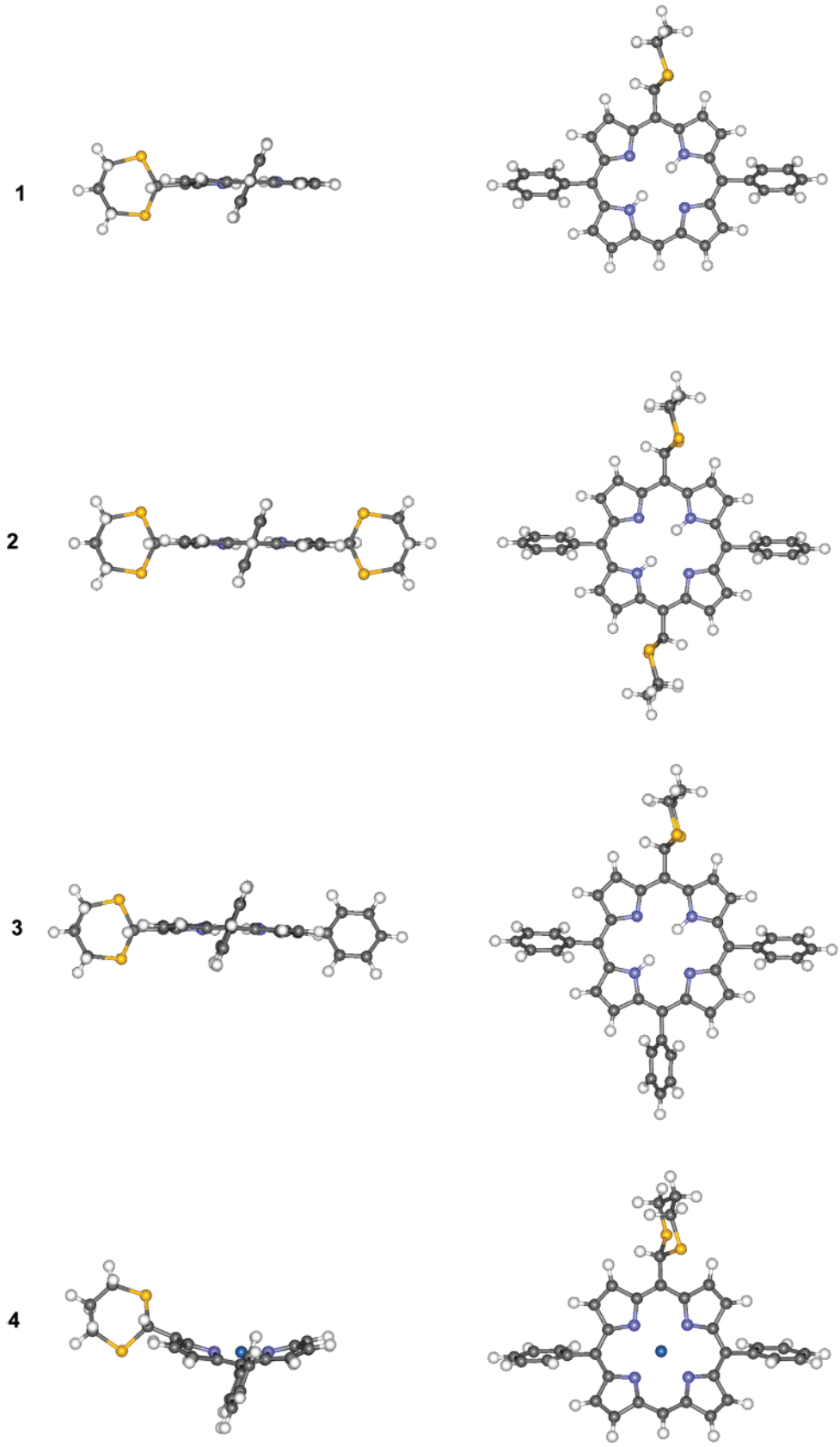

FIGURE 6. Calculated global minima structures of **1**−**4**.

substituted porphyrins) are 29−49 kJ mol^{-1}.[6,20] On the basis of this information, it can be assumed that the energy barrier should be smaller for less highly substituted porphyrins (i.e., tetrapyrroles with a smaller number of meso β peri interactions).[3c,21] To substantiate this, the transition state for the ring inversion of 5-(1,3-dithian-2-yl)porphyrinato(nickel)(II) was

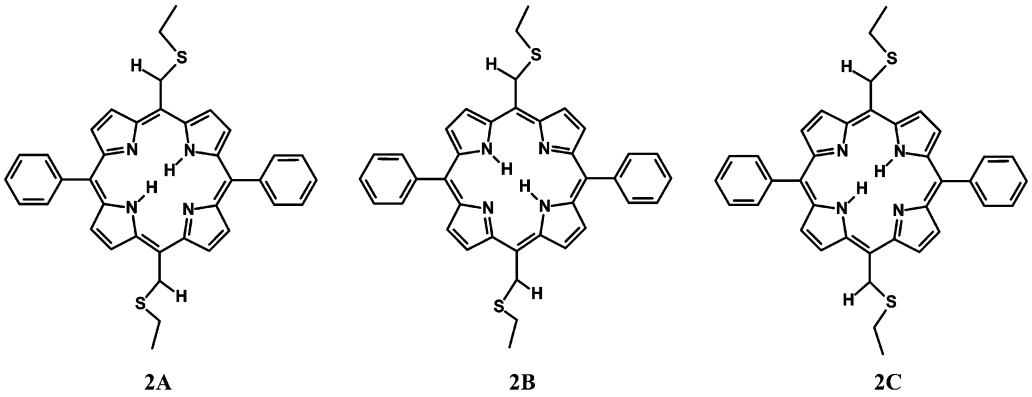

2A **2B** **2C**

FIGURE 7. Three different trans tautomers for **2**. The schematic side view of the dithianyl moieties illustrates their orientations.

TABLE 3. Activation Energies, Coalescence Temperatures, and Calculated Energy Barriers for the Dithianyl Group Rotation

		T_C (K)	ΔE (kJ·mol^{-1})	
	ΔG_{exp} (kJ·mol^{-1})	K	B3LYP/6-31G	B3LYP/6-31G[a]
1	+61.8	334	+66.8	+64.3
2	+57.3	310	+61.2	+58.8
3	+59.5	319	+62.4	+60.2
4	+47.6	258	+46.7	+44.8

[a] B3LYP + zero-point correction.

optimized. The transition state exhibits a planar conformation, and the energy barrier height for the flipping of the ruffled complex was found to be 6 kJ mol^{-1}. Thus, the macrocycle inversion of dithianyl-substituted porphyrins (in the temperature range investigated) is obviously too fast to be observed by NMR spectroscopy.

Conformation of the Dithianyl Group. The ^{1}H NMR data for the dithianyl rings indicate that these six-membered rings have a chair-type conformation and are linked in an equatorial position to the porphyrin. All ^{1}H NMR signals of the dithianyl moiety for compounds **1**−**4** remained unchanged over the temperature range from 360 to 200 K. Thus, no dynamic processes, such as chair−chair inversion, occur within the dithianyl moieties.[22]

Rotational Barriers. In contrast to the free bases **1**−**3**, the ^{1}H NMR spectra of the metal complex **4** reveal fused resonances for protons H3/H7 at 298 K. Below 258 K, a splitting occurs because of slower rotation of the *meso*-alkyl residue. This indicates that the dithianyl group can rotate more freely in the metal complex (vide supra). The calculated energy values for the rotational barriers for porphyrins **1**−**4** are in good agreement with the experimentally obtained data (Table 3). It is a long established fact that a central nickel atom imposes a *ruf* distorted core conformation through Ni−N bond contraction.[23] This aids the rotation of an aryl substituent in the meso position and lowers the rotational barrier for this process.[24]

To clarify the origin of the lower rotational barrier of the alkyl moiety in nickel complexes compared to that of free base porphyrins, we compared the macrocyclic distortions of the calculated structures **1** and **4**. As shown in Figure 8, **1** shows no significant deviations from planarity, whereas **4** exhibits significant out-of-plane deformation. However, the rotational transition states **1TS** and **4TS1** exhibit both similar out-of-plane distortions. This observation is further emphasized by a Normal-Coordinate Structural Decomposition (NSD) analysis[9,25,35] of the six lowest energy out-of-plane distortion modes for the participating species (Figure 9). The conformations of the three species **1TS**, **4**, and **4TS** all exhibit predominant contributions

(20) Waditschatka, R.; Kratky, C.; Jaun, B.; Heinzer, J.; Eschenmoser, A. *J. Chem. Soc., Chem. Commun*. **1985**, 1604−1607.

(21) (a) Medforth, C. J.; Berber, M. D.; Smith, K. M.; Shelnutt, J. A. *Tetrahedron Lett.* **1990**, *31*, 3719−3722. (b) Kalisch, W. W.; Senge, M. O. *Tetrahedron Lett.* **1996**, *37*, 1183−1186. (c) Senge, M. O.; Forsyth, T. P.; Smith, K. M. *Z. Kristallogr.* **1996**, *211*, 176−185. (d) Senge, M. O.; Kalisch, W. W. *Inorg. Chem.* **1997**, *36*, 6103−6116. (e) Senge, M. O.; Bischoff, I. *Eur. J. Org. Chem.* **2001**, 1735−1751.

(22) Kleinpeter, E. *Adv. Heterocycl. Chem.* **2004**, *86*, 41−127.

(23) (a) Hoard, J. L. *Science* **1971**, *174*, 1295−1302. (b) Hoard, J. L. *Ann. N.Y. Acad. Sci.* **1973**, *206*, 18−31. (c) Meyer, E. F., Jr. *Acta Crystallogr.* **1972**, *28*, 2162−2167. (d) Cullen, D. L.; Meyer, E. F., Jr. *J. Am. Chem. Soc.* **1974**, *96*, 2095−2102.

(24) Medforth, C. J.; Haddad, R. E.; Muzzi, C. M.; Dooley, N. R.; Jaquinod, L.; Shyr, D. C.; Nurco, D. J.; Olmstead, M. M.; Smith, K. M.; Ma, J.-G.; Shelnutt, J. A. *Inorg. Chem.* **2003**, *42*, 2227−2241.

(25) (a) Song, X.-Z.; Jentzen, W.; Jia, S.-L.; Jaquinod, L.; Nurco, D. J.; Medforth, C. J.; Smith, K. M.; Shelnutt, J. A. *J. Am. Chem. Soc.* **1996**, *118*, 12975−12988. (b) Song, X.-Z.; Jentzen, W.; Jaquinod, L.; Khoury, R. G.; Medforth, C. J.; Jia, S.-L.; Ma, J.-G.; Smith, K. M.; Shelnutt, J. A. *Inorg. Chem.* **1998**, *37*, 2117−2128.

(26) Van Geet, A. L. *Anal. Chem.* **1970**, *42*, 679−680.

(27) Gutowsky, H. S.; Holm, C. H. *J. Chem. Phys.* **1956**, *25*, 1228−1234.

(28) Frisch, M. J.; Trucks, G. W.; Schlegel, H. B.; Scuseria, G. E.; Robb, M. A.; Cheeseman, J. R.; Montgomery, J. A., Jr.; Vreven, T.; Kudin, K. N.; Burant, J. C.; Millam, J. M.; Iyengar, S. S.; Tomasi, J.; Barone, V.; Mennucci, B.; Cossi, M.; Scalmani, G.; Rega, N.; Petersson, G. A.; Nakatsuji, H.; Hada, M.; Ehara, M.; Toyota, K.; Fukuda, R.; Hasegawa, J.; Ishida, M.; Nakajima, T.; Honda, Y.; Kitao, O.; Nakai, H.; Klene, M.; Li, X.; Knox, J. E.; Hratchian, H. P.; Cross, J. B.; Bakken, V.; Adamo, C.; Jaramillo, J.; Gomperts, R.; Stratmann, R. E.; Yazyev, O.; Austin, A. J.; Cammi, R.; Pomelli, C.; Ochterski, J. W.; Ayala, P. Y.; Morokuma, K.; Voth, G. A.; Salvador, P.; Dannenberg, J. J.; Zakrzewski, V. G.; Dapprich, S.; Daniels, A. D.; Strain, M. C.; Farkas, O.; Malick, D. K.; Rabuck, A. D.; Raghavachari, K.; Foresman, J. B.; Ortiz, J. V.; Cui, Q.; Baboul, A. G.; Clifford, S.; Cioslowski, J.; Stefanov, B. B.; Liu, G.; Liashenko, A.; Piskorz, P.; Komaromi, I.; Martin, R. L.; Fox, D. J.; Keith, T.; Al-Laham, M. A.; Peng, C. Y.; Nanayakkara, A.; Challacombe, M.; Gill, P. M. W.; Johnson, B.; Chen, W.; Wong, M. W.; Gonzalez, C.; Pople, J. A. *Gaussian 03*, revision C.02; Gaussian, Inc.: Wallingford, CT, 2004.

(29) Becke, A. D. *J. Chem. Phys.* **1993**, *98*, 5648−5652.

(30) Lee, C.; Yang, W.; Parr, R. G. *Phys. Rev. B* **1988**, *37*, 785−789.

(31) Ditchfield, R.; Hehre, W. J.; Pople, J. A. *J. Chem. Phys.* **1971**, *54*, 724−728.

(32) Petersson, G. A.; Bennett, A.; Tensfeldt, T. G.; Al-Laham, M. A.; Shirley, W. A.; Mantzaris, J. *J. Chem. Phys.* **1988**, *89*, 2193−2218.

(33) Ditchfield, J. R. *Mol. Phys.* **1974**, *27*, 789−807.

(34) Cheeseman, J. P.; Trucks, G. W.; Keith, T. A.; Frisch, M. J. *J. Chem. Phys.* **1996**, *104*, 5497−5509.

(35) (a) Jentzen, W.; Song, X.-Z.; Shelnutt, J. A. *J. Phys. Chem. B* **1997**, *101*, 1684−1699. (b) Jentzen, W.; Ma, J.-G.; Shelnutt, J. A. *Biophys. J.* **1998**, *74*, 753−763.

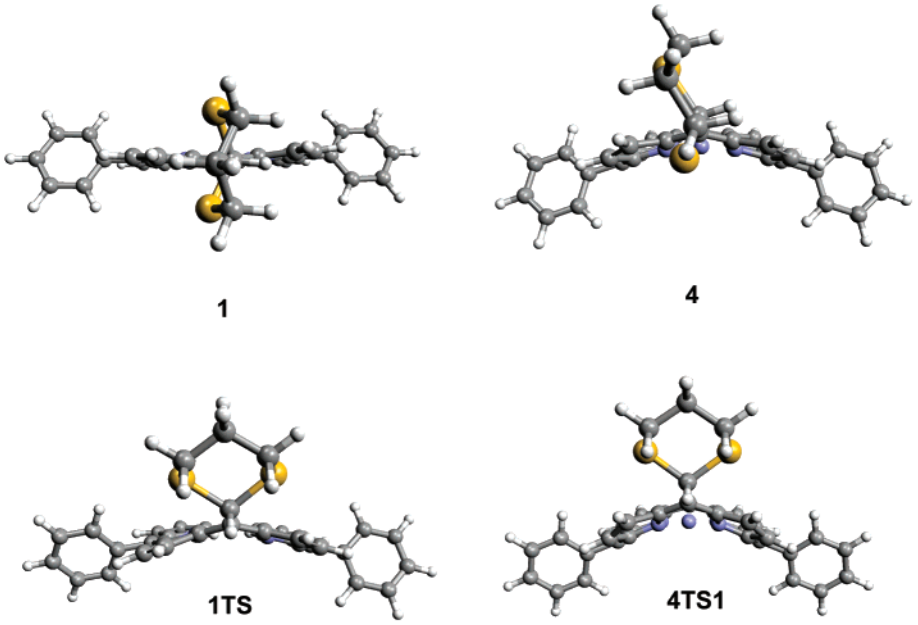

FIGURE 8. Ground and transition states for **1** and **4**.

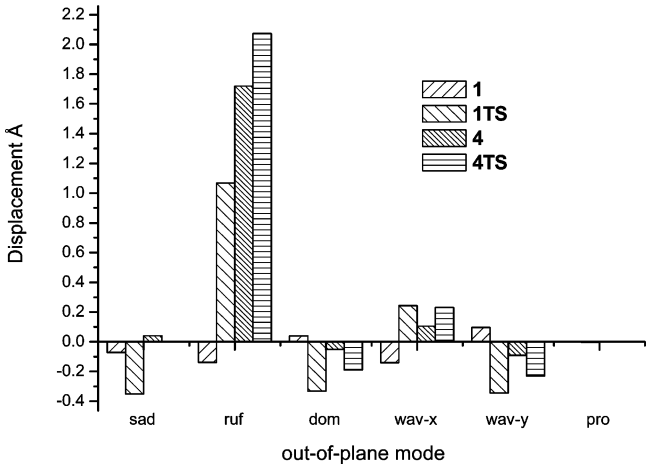

FIGURE 9. NSD analysis of **1** and **4**, ground and rotational transition states, respectively.

from *ruf* distortion. Thus, the core conformations of the ground and rotational transition states for **4** are quite similar. Hence, less energy is required for the conformational change of the porphyrin moiety during the rotation. In contrast, a higher energy is required for changing **1** to **1TS**. Overall, the similar ruffled core conformations in the ground and transition states result in a reduction of the rotational barrier by approximately 12 kJ mol^{-1}.

Conclusions

The conformational behavior of a series of *meso*-(1,3-dithian-2-yl)-substituted porphyrins has been examined by VT NMR spectroscopy and molecular modeling. A detailed analysis of the variable-temperature ^{1}H NMR data and quantum chemical calculations gave a thorough view of the conformational landscape of dithianyl porphyrins and serves as an illustrative example for the conformational flexibility of *meso*-alkylporphyrins. Thus, in the free base porphyrins **1**−**3**, the orientation of the dithianyl residue gives rise to different but energetically similar NH trans tautomers which were identified. The transition state for the dithianyl rotation about the C5−C25 bond in both the free base **1** and the nickel(II) complex **4** exhibits a severely ruffled porphyrin core conformation in both. This first description of a rotational transition state for the rotation of a bulky alkyl substituent in porphyrins indicates the necessity to expand studies on the dynamic processes in conformationally distorted porphyrins to the effects of both aryl and alkyl residues. Computational data illustrated the similarity of the porphyrin macrocycle conformation in the transition state and global minimum structure of the nickel complex **4** and gave a structural basis for the lower rotational barrier in metalloporphyrins compared to that of the free base systems. This further supports the crucial interplay between core conformation, metal effects and substituent type, orientation, and conformation on the conformational landscape of tetrapyrrole. This study therefore provides precious information about *meso*-alkyl-substituted porphyrins that have not been received before. *meso*-Alkyl-substituted porphyrins can be used furthermore as model compounds for biologically relevant systems since they show a structure similar to that of naturally occurring porphyrins.

Experimental Section

Materials. Compounds **1**−**4** were prepared as described before.[14]

NMR Studies. All NMR experiments were performed with a 500 MHz spectrometer and internally referenced to TMS. Samples were ca. 0.05 M and dissolved in dry CD_2Cl_2 for room- and low-temperature measurements and in dry $C_2D_2Cl_4$ for high-temperature investigations. The temperature was calibrated by the shift difference between the proton resonances in methanol and maintained to within ±1 K.[26] ^{1}H resonances were assigned completely by NOESY, COSY, and long-range COSY experiments using standard pulse sequences as well as at 298 and 200 K. The free energy of activation was obtained from the evaluation of the ^{1}H NMR spectra using standard procedures.[27]

Computational Studies. Quantum chemical calculations were performed on Origin2000 and 1.7 GHz Linux-based personal computer using the Gaussian 03 software package.[28] For geometry optimization of the ground-state structures and for NMR chemical shift calculations, the theory level B3LYP and basis set 6-31G** were used.[29−32] Chemical shift calculations were performed using the GIAO approach.[33,34] For energetic evaluations, the transition-state geometries and ground-state structures were calculated at the same theory level using the 6-31G basis set. The geometry optimizations of ground and transition states were performed without any symmetry restrictions and were followed by frequency calculations to verify the character of the stationary point obtained.

Normal-Coordinate Structural Decomposition. The theoretical background and development of this method has been described by Shelnutt and co-workers.[35] For calculations, we used the NSD engine program version 3.0.[36]

Acknowledgment. This work was generously supported by a Science Foundation Ireland Research Professorship Grant (SFI 04/RP1/B482).

Supporting Information Available: Additional ^{1}H NMR spectra, coordinates of optimized structures, and absolute energies. This material is available free of charge via the Internet at http://pubs.acs.org.

JO0708700

(36) Sandia National Laboratories. Normal-Coordinate Structural Decomposition Engine. http://jasheln.unm.edu/jasheln/content/nsd/NSDengine/nsd_index.htm.